

Open camera or QR reader and
scan code to access this article
and other resources online.



Epitope Mapping of an Anti-ferret Podoplanin Monoclonal Antibody Using the PA Tag-Substituted Analysis

Yu Isoda, Mika K. Kaneko, Tomohiro Tanaka, Hiroyuki Suzuki, and Yukinari Kato

In small animal models of severe acute respiratory syndrome coronaviruses (SARS-CoV and SARS-CoV-2) infection, ferrets (*Mustela putorius furo*) have been used to investigate the pathogenesis. Podoplanin (PDPN) is an essential marker in lung type I alveolar epithelial cells, kidney podocytes, and lymphatic endothelial cells. Monoclonal antibodies (mAbs) against ferret PDPN (ferPDPN) are useful for the pathological analyses of those tissues. We previously established an anti-ferPDPN mAb, PMab-292 using the Cell-Based Immunization and Screening (CBIS) method. In this study, we determined the critical epitope of PMab-292 using flow cytometry. The ferPDPN deletion mutants analysis revealed that the Val34 is located at the N-terminus of the PMab-292 epitope. Furthermore, the PA tag-substituted analysis (PA scanning) showed that Asp39 is located at the C-terminus of PMab-292 epitope. The epitope sequence (VRPEDD) also exists between Val26 and Asp31 of ferPDPN, indicating that PMab-292 recognizes the tandem repeat of the VRPEDD sequence of ferPDPN.

Keywords: ferret podoplanin, monoclonal antibody, epitope, PA scanning

Introduction

FERRETS (*MUSTELA PUTORIUS FURO*) HAVE been used as an animal model for investigating the transmission and pathogenicity of human severe acute respiratory syndrome coronaviruses (SARS-CoV¹ and SARS-CoV-2²). In histopathological analysis, inflammation within alveolar spaces and perivascular mononuclear parts were observed in SARS-CoV-2-infected ferrets. Microscopic observations of SARS-CoV-2-infected ferrets exhibited mild bronchoalveolar or alveolar inflammation.² However, there is a limitation of the pathological analysis owing to the lack of antibodies that can recognize the ferret-derived antigens and distinguish the specific cells in the lung.

Podoplanin (PDPN) is a type I transmembrane mucin-like sialoglycoprotein and an important marker in lung type I alveolar epithelial cells,^{3,4} kidney podocytes,⁵ and lymphatic endothelial cells.^{6,7} PDPN possesses a heavily glycosylated N-terminal extracellular domain, a single transmembrane domain, and a short intracellular domain.^{8,9} A repeat sequence of EDxxVTPG, named PLAG domains, is present in the N-terminal domain. “PLAG” is derived from the platelet aggregation-stimulating function of PDPN.¹⁰ Furthermore,

several PLAG-like domains (PLDs, one of which is also named PLAG4 domain) have been identified.¹¹

Anti-ferret PDPN (ferPDPN) monoclonal antibodies (mAbs) have been proposed as a useful tool to investigate the pathogenesis of lung type I alveolar epithelial cells, kidney podocytes, and lymphatic endothelial cells in SARS-CoV-2 infected ferret. We previously established an anti-ferPDPN mAb, PMab-292 using the Cell-Based Immunization and Screening (CBIS) method. PMab-292 can be used for flow cytometry, western blotting, and immunohistochemistry.¹² To clarify further characteristics of PMab-292, we performed epitope mapping using flow cytometry.

Materials and Methods

Antibodies

PMab-292 (an anti-ferPDPN mAb),¹² PMab-241 (an anti-bear PDPN mAb),¹³ PMab-1 (an anti-MAP tag mAb),¹⁴ and NZ-1 (an anti-PA tag mAb)¹⁵ were described previously. Alexa Fluor 488-conjugated anti-mouse IgG and anti-rat IgG were purchased from Cell Signaling Technology, Inc. (Danvers, MA).

Plasmid construction and transfection

Synthesized DNA (Eurofins Genomics KK, Tokyo, Japan) encoding ferPDPN plus an N-terminal MAP tag (GDGMVPPGIEDK)^{16,17} were subcloned into a pCAG-Ble vector (FUJIFILM Wako Pure Chemical Corporation, Osaka, Japan). The ferPDPN deletion mutants (dN33, dN34, dN35, dN36, dN37, dN38, dN39, dN40, dN41, dN42, and dN43) were produced using a KAPA HiFi HotStart ReadyMix polymerase chain reaction (PCR) Kit (Kapa Biosystems, Wilmington, MA), and subcloned into the pCAG-Ble vector.

For PA scanning, the substitution of PA tag (GVAMP GAEDDVV) in ferPDPN dN34 was performed with oligonucleotides containing PA tag sequence at the desired position. For example, for the substitution of the PA tag from Val34 to Asn45 of ferPDPN, we constructed Thr33-GVAMPGAEDDVV-Asn46 (₃₄-PA-₄₅) in ferPDPN dN34. The PCR fragments bearing the desired mutations were inserted into the pCAG-neo vector (FUJIFILM Wako Pure Chemical Corporation) using an In-Fusion HD Cloning Kit (Takara Bio, Inc., Shiga, Japan). Substitutions of amino acids to alanine (or glycine) in the ferPDPN sequence were conducted by QuikChange Lightning Site-Directed Mutagenesis Kits (Agilent Technologies, Inc., Santa Clara, CA). PCR fragments bearing the desired mutations were inserted into the pCAG-neo vector using the In-Fusion HD Cloning Kit (Takara Bio, Inc.).

The ferPDPN mutant plasmids were transiently transfected into Chinese hamster ovary (CHO)-K1 cells (the American Type Culture Collection, Manassas, VA) using the Neon Transfection System (Thermo Fisher Scientific, Inc., Waltham, MA). CHO-K1 cells and transfectants were cultured in Roswell Park Memorial Institute (RPMI)-1640 medium (Nacalai Tesque, Inc., Kyoto, Japan) supplemented with 10% heat-inactivated fetal bovine serum (FBS; Thermo Fisher Scientific, Inc.), 100 units/mL of penicillin, 100 µg/mL of streptomycin, and 0.25 µg/mL of amphotericin B (Nacalai Tesque, Inc.). The cells were cultured at 37°C in a humidified atmosphere containing 5% CO₂ and 95% air.

Flow cytometry

CHO-K1 cells and transfectants were harvested after a brief exposure to 0.25% trypsin in 1 mM ethylenediaminetetraacetic acid (EDTA; Nacalai Tesque, Inc.) and washed with 0.1% bovine serum albumin in phosphate-buffered saline. PMAb-292 (1 µg/mL), PMAb-241 (1 µg/mL), PMAb-1 (1 µg/mL), or NZ-1 (1 µg/mL) were incubated for 30 minutes at 4°C. The cells were further treated with Alexa Fluor 488-conjugated anti-mouse IgG or anti-rat IgG (1:1000). Fluorescence data were collected using the SA3800 Cell Analyzer (Sony Corp., Tokyo, Japan).

Results

Epitope mapping of PMAb-292 using the N-terminal deletion mutants of ferPDPN

We previously established an anti-ferPDPN mAb (PMAb-292) by the CBIS method. To determine the PMAb-292 epitope, we examined the reactivity to the N-terminal ferPDPN deletion mutants (from dN33 to dN43)-overexpressed CHO-K1 cells by flow cytometry (Fig. 1A). As shown in Figure 1B, PMAb-292 reacted with dN33 and dN34. In

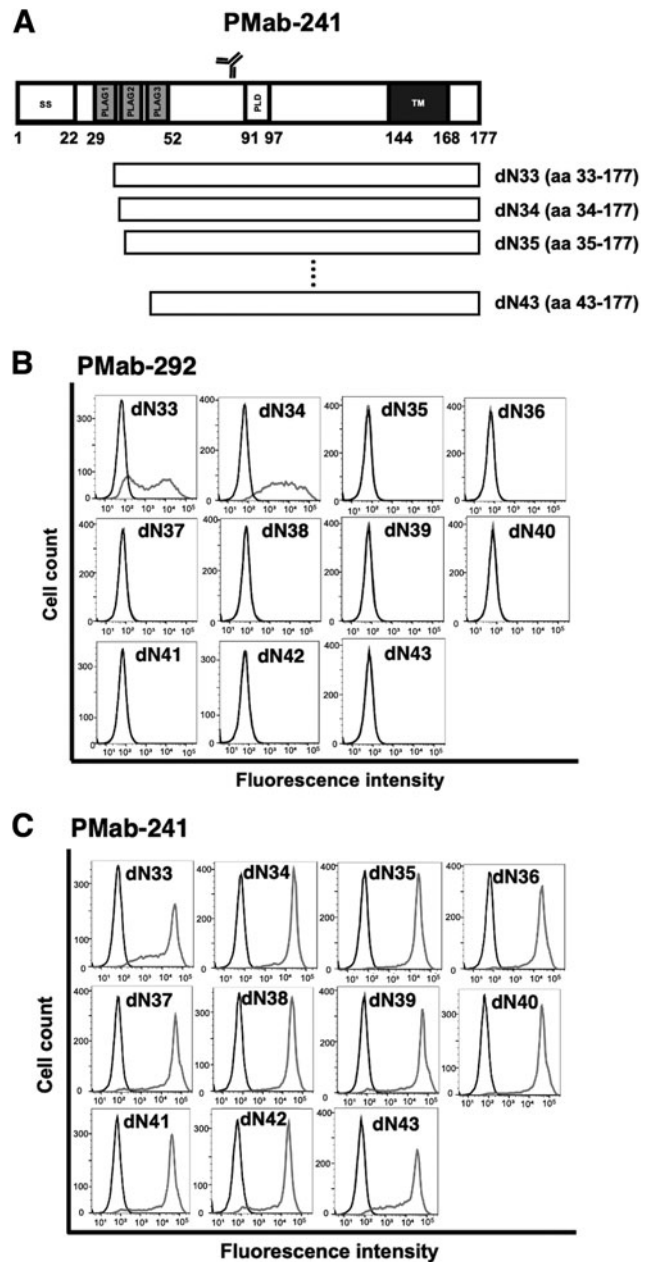


FIG. 1. Epitope determination of PMAb-292 using deletion mutants of ferPDPN. (A) The ferPDPN deletion mutants were transiently expressed in CHO-K1 cells. (B) The ferPDPN mutants-expressed CHO-K1 cells were incubated with 1 µg/mL of PMAb-292 (B, red line) or 1 µg/mL of PMAb-241 (C, red line), or control blocking buffer (black line), followed by secondary antibodies treatment. The data were analyzed using the SA3800 Cell Analyzer. CHO, Chinese hamster ovary; ferPDPN, ferret podoplanin; PLAG, platelet aggregation-stimulating; PLD, PLAG-like domain; ss, signal sequence; TM, transmembrane domain.

contrast, the reactivity completely disappeared in dN35, dN36, dN37, dN38, dN39, dN40, dN41, dN42, and dN43. We confirmed the cell surface expression of all deletion mutants using PMAb-241, originally developed as an anti-ferPDPN mAb, which cross-reacts with ferPDPN (epitope amino acids: Thr86, Asp87, and Arg89).¹⁸ These results indicated that the Val34 is located at the N-terminus of PMAb-292 epitope.

To identify the binding epitope of PMAb-292, we generated 20 alanine (or glycine)-substituted ferPDPN (Supplementary Fig. S1A) and investigated the reactivity of PMAb-292 against CHO-K1 cells, which overexpressed the ferPDPN mutants transiently. PMAb-292 reacted with all alanine (or glycine)-substituted mutants and wild type (WT) (Supplementary Fig. S1B). We also examined the reactivity of PMAb-292 against 2×alanine (or glycine)-substituted ferPDPN (Supplementary Fig. S2A); however, PMAb-292 reacted with all mutants (Supplementary Fig. S2B). There-

fore, we could not determine the epitope of PMAb-292 using 1×alanine or 2×alanine scanning methods.

Flow cytometry using PMAb-292 with PA tag-substituted ferPDPN

As shown in Figure 1B, PMAb-292 reacted with the ferPDPN dN34 mutant. We next generated PA tag (GVAMPGAEDDVV)-substituted ferPDPN dN34 mutants as shown in Figure 2A to determine the C-terminus of the PMAb-292

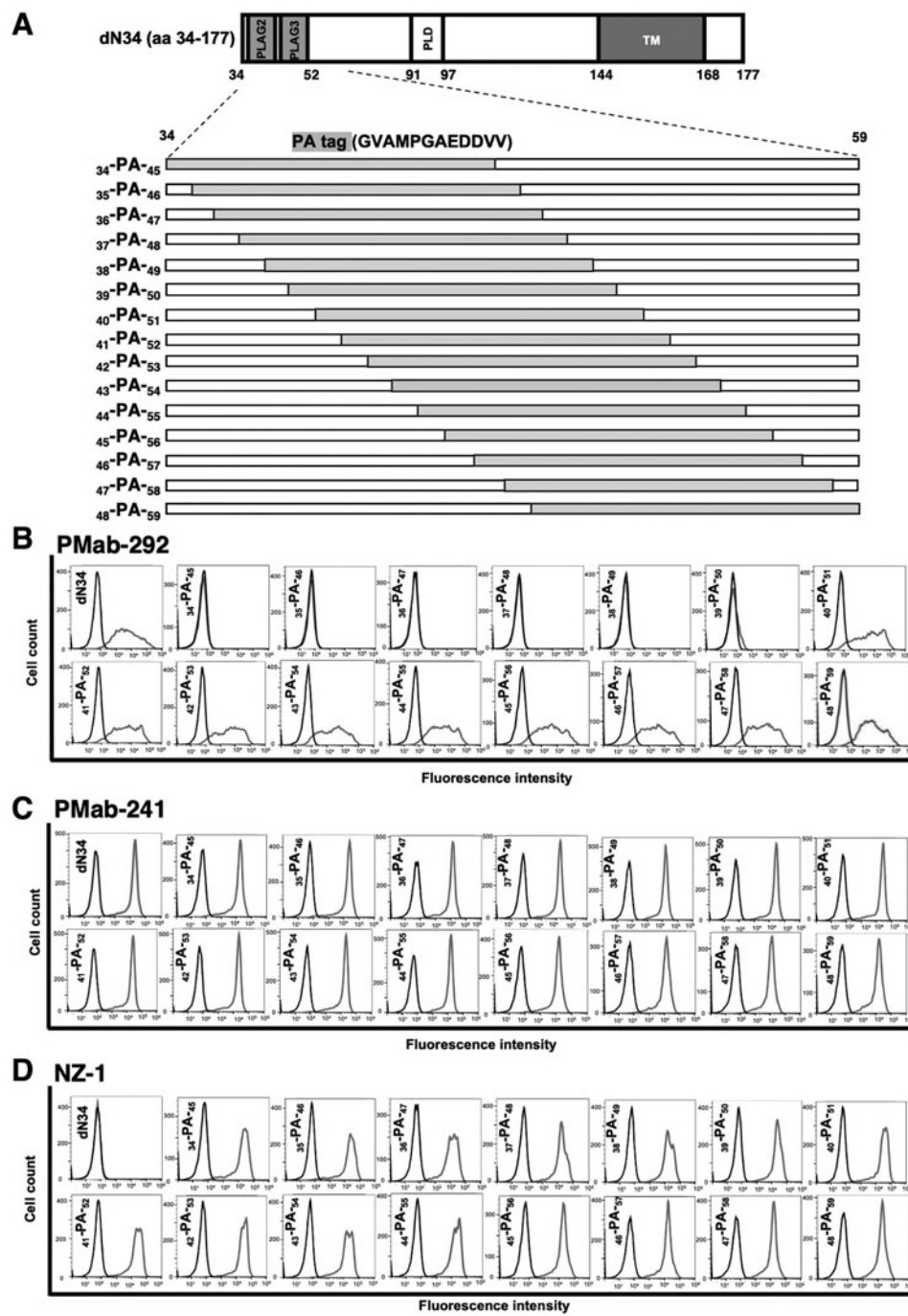


FIG. 2. Epitope determination of PMAb-292 using PA tag-substituted mutants of ferPDPN. (A) The ferPDPN dN34 PA tag-substituted mutants were transiently expressed in CHO-K1 cells. (B) The mutants-expressed CHO-K1 cells were incubated with 1 μg/mL of PMAb-292 (B, red line), 1 μg/mL of PMAb-241 (C, red line), 1 μg/mL of NZ-1 (D, red line), or control blocking buffer (black line), followed by secondary antibodies treatment. The data were analyzed using the SA3800 Cell Analyzer.

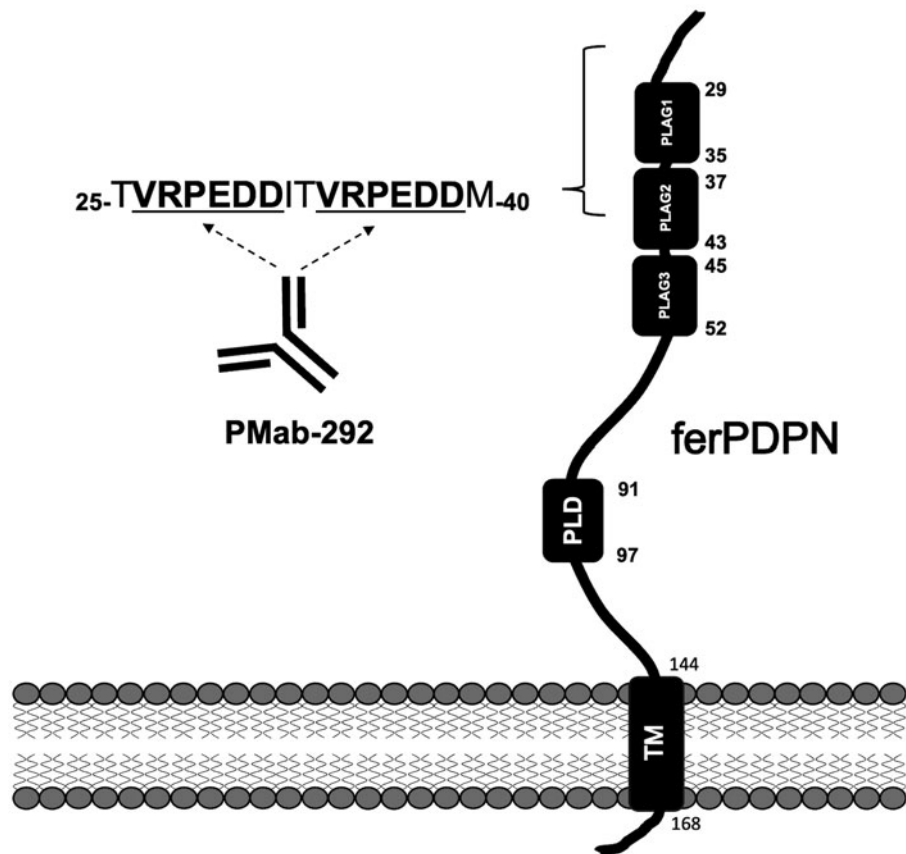


FIG. 3. Schematic illustration of ferPDPN and the PMab-292 epitope. The PMab-292 epitope involves tandem sequence (VRPEDD) of ferPDPN. PLAG, platelet aggregation-stimulating; PLD, PLAG-like domain; TM, transmembrane domain.

epitope. As shown in Figure 2B, the reactivity of PMab-292 almost completely disappeared in $_{34}$ -PA- $_{45}$, $_{35}$ -PA- $_{46}$, $_{36}$ -PA- $_{47}$, $_{37}$ -PA- $_{48}$, $_{38}$ -PA- $_{49}$, and $_{39}$ -PA- $_{50}$ mutants of ferPDPN dN34. In contrast, the reactivity of PMab-292 was observed in the substituted mutants from 40th to 59th amino acids. These results indicated that the epitope of PMab-292 contains the $_{34}$ -VRPEDD- $_{39}$ sequence of ferPDPN.

Discussion

In this study, we performed the flow cytometry-mediated epitope mapping of PMab-292 using ferPDPN deletion mutants (Fig. 1) and PA scanning of ferPDPN (Fig. 2). We found that $_{34}$ -VRPEDD- $_{39}$ sequence of ferPDPN is an important sequence of PMab-292 epitope. In contrast, we could not identify the critical amino acids using $1 \times$ Ala scanning (Supplementary Fig. S1) or $2 \times$ Ala scanning (Supplementary Fig. S2) using flow cytometry. Figure 3 shows the surrounding sequence of $_{34}$ -VRPEDD- $_{39}$, and found that the same VRPEDD sequence is present between the 26th and 31st amino acids of ferPDPN. This might be the reason why we could not determine the critical amino acids of the ferPDPN epitope using $1 \times$ Ala scanning and $2 \times$ Ala scanning in the $_{34}$ -VRPEDD- $_{39}$ sequence. In other words, PMab-292 probably recognizes the tandem sequences from PLAG1 to PLAG2 domains (Fig. 3). Therefore, the alanine-substitution of two same amino acids in both $_{26}$ -VRPEDD- $_{31}$ and $_{34}$ -VRPEDD- $_{39}$ sequence is essential to determine the critical amino acids of PMab-292 epitope.

PLAG domains play a critical role in platelet aggregation. In humans, the *O*-glycosylation in PLAG3 or PLD is crucial for PDPN-induced platelet aggregation.^{19,20} A platelet receptor, CLEC-2 recognizes the sialylated PLAG3 or PLDs of PDPN, which is essential for PDPN-induced platelet aggregation. We have not examined whether ferPDPN can induce platelet aggregation and have not determined the essential *O*-glycosylated amino acids for platelet aggregation in PLAG domains. However, PMab-292 could contribute to the study of platelet aggregation by ferPDPN.

We have determined the epitopes of anti-PDPN mAbs against various species.¹¹ It is the first example that the tandem sequence is recognized by an anti-PDPN mAb. We performed immunohistochemistry using PMab-292 and could detect kidney podocytes and lung alveolar epithelial cells with high sensitivity.¹² The property of PMab-292 may contribute to the high sensitivity of immunohistochemical analysis, which is important for the pathological analysis of lung injury by SARS-CoVs.

Authors' Contributions

Y.I. and T.T. performed the experiments. M.K.K. and Y.K. designed the experiments. Y.I. and M.K.K. analyzed the data. H.S. and Y.K. wrote the manuscript. All authors have read and agreed to the published version of the manuscript.

Author Disclosure Statement

The authors have no conflict of interest.

Funding Information

This research was supported in part by Japan Agency for Medical Research and Development (AMED) under Grant Numbers: JP23ama121008 (to Y.K.), JP23am0401013 (to Y.K.), 23bm1123027h0001 (to Y.K.), and JP23ck0106730 (to Y.K.), and by the Japan Society for the Promotion of Science (JSPS) Grants-in-Aid for Scientific Research (KAKENHI) grant numbers 21K20789 (to T.T.), 22K06995 (to H.S.), 21K07168 (to M.K.K.), and 22K07224 (to Y.K.).

Supplementary Material

Supplementary Figure S1
 Supplementary Figure S2

References

1. van den Brand JM, Haagmans BL, van Riel D, et al. The pathology and pathogenesis of experimental severe acute respiratory syndrome and influenza in animal models. *J Comp Pathol* 2014;151:83–112; doi: 10.1016/j.jcpa.2014.01.004
2. Muñoz-Fontela C, Dowling WE, Funnell SGP, et al. Animal models for COVID-19. *Nature* 2020;586:509–515; doi: 10.1038/s41586-020-2787-6
3. Dobbs LG, Williams MC, Gonzalez R. Monoclonal antibodies specific to apical surfaces of rat alveolar type I cells bind to surfaces of cultured, but not freshly isolated, type II cells. *Biochim Biophys Acta* 1988;970:146–156; doi: 10.1016/0167-4889(88)90173-5
4. Rishi AK, Joyce-Brady M, Fisher J, et al. Cloning, characterization, and development expression of a rat lung alveolar type I cell gene in embryonic endodermal and neural derivatives. *Dev Biol* 1995;167:294–306; doi: 10.1006/dbio.1995.1024
5. Breiteneder-Geleff S, Matsui K, Soleiman A, et al. Podoplanin, novel 43-kd membrane protein of glomerular epithelial cells, is down-regulated in puromycin nephrosis. *Am J Pathol* 1997;151:1141–1152.
6. Hirakawa S, Hong YK, Harvey N, et al. Identification of vascular lineage-specific genes by transcriptional profiling of isolated blood vascular and lymphatic endothelial cells. *Am J Pathol* 2003;162:575–586; doi: 10.1016/s0002-9440(10)63851-5
7. Petrova TV, Mäkinen T, Mäkelä TP, et al. Lymphatic endothelial reprogramming of vascular endothelial cells by the Prox-1 homeobox transcription factor. *EMBO J* 2002; 21:4593–4599; doi: 10.1093/emboj/cdf470
8. Krishnan H, Rayes J, Miyashita T, et al. Podoplanin: An emerging cancer biomarker and therapeutic target. *Cancer Sci* 2018;109:1292–1299; doi: 10.1111/cas.13580
9. Quintanilla M, Montero-Montero L, Renart J, et al. Podoplanin in inflammation and cancer. *Int J Mol Sci* 2019;20: 707; doi: 10.3390/ijms20030707
10. Kato Y, Fujita N, Kunita A, et al. Molecular identification of Aggrus/T1alpha as a platelet aggregation-inducing factor expressed in colorectal tumors. *J Biol Chem* 2003;278: 51599–51605; doi: 10.1074/jbc.M309935200
11. Suzuki H, Kaneko MK, Kato Y. Roles of podoplanin in malignant progression of tumor. *Cells* 2022;11:575; doi: 10.3390/cells11030575
12. Goto N, Suzuki H, Tanaka T, et al. Development of a monoclonal antibody PMab-292 against ferret podoplanin. *Monoclon Antib Immunodiagn Immunother* 2022;41:101–109; doi: 10.1089/mab.2021.0067
13. Takei J, Yamada S, Konnai S, et al. PMab-241 specifically detects bear podoplanin of lymphatic endothelial cells in the lung of brown bear. *Monoclon Antib Immunodiagn Immunother* 2019;38:282–284; doi: 10.1089/mab.2019.0038
14. Kaji C, Tsujimoto Y, Kaneko MK, et al. Immunohistochemical examination of novel rat monoclonal antibodies against mouse and human podoplanin. *Acta Histochem Cytochem* 2012;45:227–237; doi: 10.1267/ahc.12008
15. Kato Y, Kaneko MK, Kuno A, et al. Inhibition of tumor cell-induced platelet aggregation using a novel anti-podoplanin antibody reacting with its platelet-aggregation-stimulating domain. *Biochem Biophys Res Commun* 2006; 349:1301–1307; doi: 10.1016/j.bbrc.2006.08.171
16. Fujii Y, Kaneko MK, Kato Y. MAP tag: A novel tagging system for protein purification and detection. *Monoclon Antib Immunodiagn Immunother* 2016;35:293–299; doi: 10.1089/mab.2016.0039
17. Wakasa A, Kaneko MK, Kato Y, et al. Site-specific epitope insertion into recombinant proteins using the MAP tag system. *J Biochem* 2020;168:375–384; doi: 10.1093/jb/mvaa054
18. Sayama Y, Sano M, Asano T, et al. Epitope mapping of PMab-241, a lymphatic endothelial cell-specific anti-bear podoplanin monoclonal antibody. *Monoclon Antib Immunodiagn Immunother* 2020;39:77–81; doi: 10.1089/mab.2020.0004
19. Kaneko MK, Kato Y, Kameyama A, et al. Functional glycosylation of human podoplanin: Glycan structure of platelet aggregation-inducing factor. *FEBS Lett* 2007;581: 331–336; doi: 10.1016/j.febslet.2006.12.044
20. Sekiguchi T, Takemoto A, Takagi S, et al. Targeting a novel domain in podoplanin for inhibiting platelet-mediated tumor metastasis. *Oncotarget* 2016;7:3934–3946; doi: 10.18632/oncotarget.6598

Address correspondence to:

Yukinari Kato
 Department of Antibody Drug Development
 Tohoku University Graduate School of Medicine
 2-1, Seiryomachi, Aoba-ku
 Sendai
 Miyagi 980-8575
 Japan

E-mail: yukinari.kato.e6@tohoku.ac.jp

Received: November 27, 2023

Accepted: December 11, 2023